Journal of Computers Vol. 37 No. 4, August 2026, pp. 255-273
https://doi.org/10.63367/19911599202608370401 5

UAV Formation Stability Control Strategy Based on Improved Radial Basis Function

Xin-Qian Fan[1,2*], Wei-Min Liu[1], Yan Zhou[1], Mei Han[1], and Juan Zhao[1]

[1] Hebei Mechanical and Electrical Polytechnic,
Xingtai City 054000, Hebei Province, China

[2] Xingtai Unmanned Aerial Vehicle Application Technology Innovation Center,
Xingtai City 054000, Hebei Province, China

fanxinqian@hbjd.edu.cn, weimin78687@126.com, 17732993731@163.com,
18803193968@163.com, d254470670@163.com

Received 9 February 2026; Revised 1 August 2026; Accepted 24 August 2026

Abstract. Stable formation control of multiple unmanned aerial vehicles (UAVs) is extremely challenging in practical missions due to factors such as strong nonlinearity, parameter fluctuations, wind disturbances, and communication between UAVs under constrained conditions. This paper proposes a distributed formation stabilization strategy, in which each UAV generates a local formation error based solely on information from its neighbors, and derives control measures from a consistent second-order error dynamic. To compensate for unknown nonlinear terms and unconsidered dynamic characteristics, an improved radial basis function (RBF) algorithm is integrated into the controller. Compared to traditional fixed-core RBF networks, the proposed method uses normalized basis functions to constrain the regressor, introduces a real-time width adjustment mechanism to improve approximation accuracy under time-varying uncertainties, and employs a robust drift learning law with leaky projection to prevent parameter divergence under stable perturbations. All closed-loop signals remain bounded, and the generated errors eventually become uniformly bounded. This paper defines a clear bound related to the approximate residual and the perturbation level. Comparative simulation results under mass disturbances, gusts, and topology changes show that the proposed method has faster convergence speed, lower steady-state generation error, and lower power consumption compared to distributed controllers without neural compensation and standard adaptive methods based on radial basis functions.

Keywords: UAV formation control, improved RBF neural network, adaptive control, distributed control, Lyapunov stability, disturbance rejection

1 Introduction

1.1 Background and Motivation

Collaborative formation control has emerged as a key technology for multi-UAV missions, particularly in situations where the spatial coverage, sensor redundancy, or mission performance of a single platform is insufficient [1]. Typical application scenarios include large-area surveillance and search, distributed inspection of linear infrastructure, and collaborative transport or relay communication, where multiple UAVs must maintain predefined geometric relationships while tracking a moving target. Compared to tracking individual UAVs, formation stabilization introduces additional communication constraints: Each UAV must not only follow the desired flight path but also compensate for relative positional deviations from neighboring or preceding UAVs, leading to the propagation of short-term coordination errors throughout the network [2]. In practical applications, formation control is also affected by several non-ideal factors [3]. First, UAV dynamics are highly nonlinear and often understeered; Even when using a progressive outer-loop control model, uncertainties such as mass changes, changes in drag, and actuator performance degradation cannot be neglected [4]. Second, wind disturbances and gusts continuously excite the closed-loop control system, which can lead to steady-state deviations or parameter drift in adaptive systems [5]. Third, the interaction of multiple agents is subject to limited communication and sensor capabilities: the topology can change due to distance limitations or packet loss, and each drone can

* Corresponding Author

typically only access information from neighboring drones and cannot determine the overall state [6]. These factors, taken together, necessitate that the shape control system exhibits distributed properties, is robust against uncertainties and disturbances, and is secured by strong stability guarantees.

1.2 Related Work

The stability and control of UAV formations have been extensively studied using advanced neural network-based strategies, particularly radial basis function neural networks (RBFNN). Peng et al. [7] introduced a robust back stepping sliding mode control (BSMC) integrated with an adaptive RBFNN to enhance attitude control of a novel coaxial eight-rotor UAV, demonstrating increased robustness against disturbances and model uncertainties. Similarly, He et al. [8] improved the control stability and accuracy of quad tiltrotor UAVs by employing an active disturbance rejection control (ADRC) with a self-tuning RBF neural network, which effectively approximates nonlinearities and enhances disturbance rejection capabilities. Fault tolerance and finite-time convergence are critical for UAV formation stability. Wang and Du [9] developed a fault-tolerant control (FTC) strategy utilizing an RBFNN-based fault estimation observer, ensuring reliable attitude control despite actuator faults and saturation. Furthermore, Pal et al. [10] proposed a dual closed-loop, fast integral terminal sliding mode control method for multi-underactuated systems, achieving finite-time convergence of formation errors and robustness against environmental disturbances, which is essential for maintaining formation stability under uncertain conditions. Adaptive and finite-time control strategies have also been extended to multi-agent UAV systems. Wang et al. [11] introduced a fully distributed, finite-time reconfiguration controller that addresses inter-UAV collision avoidance through potential energy functions, facilitating dynamic formation adjustments in response to moving leaders. In the context of under actuated vessels, Zhang et al. [12] designed a distributed adaptive formation control based on fast finite-time theory, accommodating unknown disturbances and partial nonlinearities, which can be adapted for UAV formations requiring rapid convergence and robustness. Robust control frameworks combining model predictive control (MPC) with disturbance observers have been explored to enhance formation stability. Yan et al. [13] integrated a Kalman-consensus filter with an improved MPC (IMPC) and a fixed-time disturbance observer, effectively fusing noisy data and ensuring asymptotic stability in multi-UAV formations. This approach enhances the resilience of formation control strategies in complex environments. Recent research also emphasizes cooperative control under communication constraints. Fei et al. [14] proposed a local communication-based cooperative architecture to optimize UAV observation strategies during search missions, which is vital for maintaining formation coherence when communication is limited. Bai et al. [15] extended the formation control paradigm to heterogeneous UAV-USV systems, addressing the challenges posed by unknown fractional-order dynamics and disturbances, thereby broadening the applicability of formation stability strategies. In summary, the integration of improved neural network techniques, finite-time convergence methods, and robust adaptive control strategies has significantly advanced UAV formation stability control. These approaches collectively enhance the system's ability to maintain formation integrity amidst uncertainties, disturbances, and operational constraints, providing a solid foundation for future development of UAV formation control strategies based on improved radial basis function methodologies.

1.3 Problem Statement and Research Gaps

Although distributed formation tracking, adaptive control, and robust control have been extensively studied, a significant gap remains between theoretical stability guarantees and robust formation performance under practical uncertainty. Many existing studies integrate radial basis function (RBF)-based neural networks into distributed formation controllers to approximate unknown nonlinear dynamics. However, if traditional RBF compensation is directly embedded into a formation control framework without structural improvements, several practical limitations may arise. First, the RBF regressor size can increase sharply during transient maneuvers, especially when the UAV state temporarily deviates from the nominal operating range. Such short-term regressor peaks can make the learning process overly sensitive to state changes, increasing the upper bound on uncertainty compensation and, consequently, leading to a more conservative stability boundary. Second, persistent wind disturbances, unaccounted for aerodynamic effects, actuator imperfections, and measurement noise can continually impact the adaptive update process. If the weighting law lacks an effective drift-proofing mechanism, the estimated parameters can drift slowly over time, leading to increased parameter norms, degraded steady-state tracking performance, and even unnecessary control overhead. Third, unlike single-agent systems,

trajectory generation systems are inherently interconnected through communication topologies and relative state constraints. Consequently, an approximation error in one drone can influence neighboring drones through the interconnected structure of trajectory generation systems, leading to the propagation of local errors throughout the network. Thus, the overall stability of trajectory generation and the ultimate tracking limit depend not only on the nominal feedback design but also on whether the neural approximation error, residual disturbances, and parameter estimation errors can be effectively constrained. Based on these results, this paper develops an improved trajectory generation controller in which the RBF approximator is not simply added as an additional compensation term, but is structurally redesigned to better meet the requirements of distributed drone trajectory generation control. Specifically, the proposed design introduces a normalized baseline regressor to suppress transient regressor peaks and constrain the neural network inputs during aggressive maneuvers. Simultaneously, online width adjustment is used to improve the approximation accuracy under time-varying uncertainty. This allows the RBF network to more flexibly respond to operational state changes or coordination errors. Furthermore, leakage-based learning mechanisms, as well as projection-based or constraint-based learning methods, are integrated into the adaptive weight update law to explicitly prevent parameter drift under long-term disturbances. These mechanisms ensure that the regressor, adaptive weights, and approximation residuals remain bounded in the operating domain, thereby improving both dynamic coordination behavior and steady-state stability. Finally, this paper presents a rigorous Lyapunov-based stability analysis for the resulting distributed control system. The proof demonstrates that the filtered formation error and the neural network parameter estimation error are ultimately uniformly bounded, and that the proposed controller can ensure stable formation tracking even under nonlinear uncertainties, approximation residuals, and external disturbances. Thus, the main contribution of this paper lies not only in the use of RBF neural networks for uncertainty approximation but also in the development of a bounded, drift-tolerant, and robust neural compensation framework for distributed UAV formation control.

1.4 Contributions

The main achievements of this paper are summarized as follows: Development of a Distributed Shaping Controller: A distributed shaping tracking controller is developed for a multi-agent UAV system with a second-order translational mechanics description containing unknown nonlinearities and bounded perturbations. Each agent only needs information from its neighbors to calculate the local shaping error and generate control variables. Improved RBF Compensation Mechanism: An improved RBF approximation module is proposed, which (i) incorporates normalized basis functions to ensure the boundedness of the regressor in the transient phase; (ii) employs online width adjustment to improve the approximation quality under time-varying uncertainties; and (iii) performs leakage/projection-based weight updates to minimize parameter drift under robust perturbations. High Robustness Guarantee Based on Quantitative Performance Evaluation: Analysis based on Lyapunov functions proves the closed-loop boundedness and shows that the generation error is uniformly bounded. Explicit upper bounds are applied to the approximate residuals and perturbation levels. Comparative simulations under gusts, parameter perturbations, and topology changes verify its robustness and performance advantages relative to representative benchmark models.

2 Prerequisites and Problem Description

2.1 Communication Graph and Basic Symbols

Information exchange between UAVs is modeled by a directed communication graph [16]. Each follower constructs its local formation error using only neighbor information, which supports scalable distributed implementation.

$$G = (V, E), V = \{1, 2, \ldots, N\} \tag{1}$$

Where G denotes the directed communication graph. The set V denotes the node set that contains all UAV indices, and E denotes the directed edge set that represents information links. The integer N denotes the total number of UAVs.

$$N_i = \{ j \in V | (j,i) \in E \} \tag{2}$$

Where N_i denotes the neighbor set of UAV i. The notation $(j,i) \in E$ indicates that a directed communication link exists from UAV j to UAV i, meaning that UAV i can receive information from UAV j.

$$A = [a_{ij}] \in R^{N \times N} \tag{3}$$

A denotes the adjacency matrix associated with the communication graph. The entry a_{ij} denotes the coupling weight of the directed link from j to i. If no such link exists, then a_{ij} is set to zero. The space $R^{N \times N}$ indicates that A is an N-by-N real-valued matrix.

$$d_i = \sum_{j=1}^{N} a_{ij}, D = diag(d_1, \ldots, d_N) \tag{4}$$

Where d_i denotes the in-degree of node i, defined as the sum of incoming adjacency weights. The matrix D denotes the in-degree matrix, constructed as a diagonal matrix whose diagonal entries are d_1 through d_N. The operator *diag* forms a diagonal matrix from the given scalars.

$$L = D - A \tag{5}$$

Where L denotes the Laplacian matrix of the directed graph. It is defined as the difference between the in-degree matrix D and the adjacency matrix A. To incorporate a leader agent, a pinning mechanism is introduced so that only a subset of followers needs direct access to leader information.

$$B = diag(b_1, \ldots, b_N), b_i \geq 0 \tag{6}$$

Where B denotes the pinning matrix. The scalar b_i denotes the pinning gain of follower i. The follower communication graph contains a spanning tree rooted at the leader through pinned nodes. This assumption ensures that leader information can be propagated to all followers through local interactions and enables distributed leader–follower formation tracking.

2.2 UAV Outer-Loop Dynamics with Uncertainties

The formation stabilization problem is addressed at the translational outer-loop level [17]. Unknown nonlinearities and external disturbances are explicitly included to reflect realistic operating conditions.

$$\dot{p}_i = v_i \tag{7}$$

Where $\dot{p}_i$ denotes the position vector of UAV i, and v_i denotes the velocity vector of UAV i. The dot operator denotes differentiation with respect to time.

$$\hat{fi}(x_i) = W_i^{\mathrm{T}} \Phi_i(x_i) \tag{8}$$

Where f denotes an unknown smooth nonlinear term that captures modeling uncertainties and unmodeled dynamics. The matrix B_i denotes a known and nonsingular input matrix that maps the control input to the acceleration channel. The vector u_i denotes the control input of UAV i. The disturbance $d_i(t)$ denotes an external perturbation such as wind gusts and is allowed to be time-varying.

2.3 Formation Objective and Distributed Error Construction

The desired formation is defined by a constant relative displacement vector: for each subsequent UAV, the target geometry is defined by its predefined displacement relative to neighboring UAVs. If a lead UAV is present, the target geometry is also defined by its predefined displacement relative to the lead UAV. Each UAV generates a local position error in the formation by calculating the deviation between its current relative position relative to each neighboring UAV and its corresponding target displacement relative to the neighboring UAV. If a UAV is coupled with a lead UAV, an additional term is needed to measure the deviation between its current relative position relative to the lead UAV and its target displacement. This construction method is fully distributed because it only requires the position of each UAV and the position information received from neighboring UAVs, without any global state. For controller synthesis and stability analysis, the local formation error is first-order filtered: the filtered error variable is a combination of the rate of change of the local formation error over time and a positive gain. This filtered variable allows for a convenient and dynamic representation of the control error in the Lyapunov analysis. Typically, the convergence rate is controlled through parameter optimization. The goal of this control system is to generate distributed input signals for each UAV based only on locally available information, thus ensuring that all control signals are bounded. Ideally, the generation error should converge to zero; otherwise, given bounded perturbations and approximate residuals, the error should converge to zero within a certain range. To further achieve this goal, the formation control system design also considers the interaction between local coordination errors and system uncertainties. Since the movement of each drone is subject to unknown nonlinear dynamics, external wind disturbances, and potential communication errors, the controller must be able to compensate for these effects without relying on central information. Therefore, the local filtered error is used not only as a feedback signal but also as a key variable for adaptive compensation and robust correction. As the filtered error increases, the controller intensifies its corrective actions to minimize the deviation between the actual and desired formation geometry. As the error decreases, the control input is smoothly adjusted to avoid unnecessary oscillations and excessive actuator loads. This design is particularly well-suited for distributed formation tracking, as each drone can update its control input solely based on its own state, relative information from neighboring drones, and, if available, information from the lead drone. In the case of local disturbances and approximation errors, the stability analysis should show that all signals of the closed-loop control system remain localized and that the reference error eventually converges in a compact region around the origin. This ensures a practical balance between coordination accuracy, robustness, and feasibility.

3 Improved RBF Approximation Scheme

Since audio signals are inherently context-dependent, the ability to model temporal dependencies directly impacts model performance. Chapter 3 of the references compares the advantages and disadvantages of various neural network techniques in temporal modeling. While traditional recurrent neural networks can model long-term dependencies, their hidden state update process relies on sequentially passing information from previous time steps, hindering efficient parallelization of learning and inference. In contrast, temporal convolutional neural networks (TCNs) continuously expand the receptive field by extending convolutions, significantly improving computational efficiency while maintaining contextual modeling capabilities. Therefore, this study employs multi-scale TCNs as the primary temporal modeling strategy in model optimization. To enhance information retrieval capabilities across different time scales, the references introduce a multi-scale design in the residual module, rather than relying on a single convolutional scale. This enables the model to detect local changes in adjacent frames and capture long-term dependencies. This improvement is particularly important for speech enhancement in non-stationary noise environments. This is because real-world sounds exhibit characteristics such as suddenness, gradation, and multiple overlapping sound sources, making it difficult to perform complete single-scale modeling using only convolutions. On the other hand, residual structures can improve the propagation of deep features, alleviate the performance degradation that may occur as network depth increases, and achieve more efficient transmission of temporal information between layers. Therefore, the key to optimizing temporal modeling in this chapter can be summarized as: shifting from recursive modeling to convolutional modeling, from single-scale to multi-scale, and from single-step feature propagation to deep propagation using residual structures.

3.1 Standard RBF Neural Network Approximation

Consider an unknown smooth nonlinear mapping that enters the acceleration channel of UAV i. It is approximated by an RBF network with a linear parameter structure.

$$\hat{fi}(x_i) = W_i^{\mathrm{T}} \Phi_i(x_i) \tag{9}$$

Where $\hat{fi}(x_i)$ denotes the neural estimate of the unknown nonlinear term associated with UAV i. The vector x_i denotes the local state used as the network input, typically formed by stacking the position and velocity of UAV i. The matrix W collects the adjustable weights, and the vector Φ_i collects the basis functions evaluated at x_i. A conventional Gaussian basis is used to construct the regressor.

$$\Phi_{ik}(x_i) = exp(-\frac{\left\| x_i - c_{ik} \right\|^2}{\sigma_{ik}^{\ 2}}), k = 1, 2, \ldots, M \tag{10}$$

Where $\Phi_{ik}(x_i)$ is the k-th basis output for UAV i. The vector c_{ik} is the center of the k-th Gaussian kernel, and $\sigma_{ik}^{\ 2}$ is its width. The integer M is the number of kernels. Under standard universal approximation arguments, for a compact region of interest of the state space, the unknown nonlinearity can be represented by an ideal set of weights plus a bounded residual.

$$f_i(x_i) = W_i^{*\top} \Phi_i(x_i) + \varepsilon_i(x_i) \tag{11}$$

Where $W_i^{*\top}$ denotes an ideal constant weight matrix and $\varepsilon_i(x_i)$ denotes the approximation residual caused by finite basis size and imperfect kernel placement. In practical analysis, the residual is assumed to be bounded within the operating domain.

$$\left\| \varepsilon_i(x_i) \right\| \le \overline{\varepsilon}_i \tag{12}$$

Where $\overline{\varepsilon}_i$ denotes a positive constant bound on the residual magnitude. While the baseline structure is widely used, two practical issues frequently appear in formation control applications: the regressor magnitude can become spiky during transients, and the weight adaptation can drift under persistent disturbances. The following subsections address these issues by modifying both the basis construction and the adaptation mechanism.

3.2 Proposed Improved RBF Design

The improved RBF design proposed in this paper enhances the online uncertainty compensation capability of formation control under transient and persistent disturbances by combining three practical mechanisms in Table 1. First, a simple scaling is used to normalize the basis function regressor, ensuring that the mapping relationship between the network input and the regressor remains bounded even if the UAV state temporarily deviates from the nominal working area; this prevents transient spikes from causing overly aggressive learning or overly conservative stability limits. Second, instead of using a fixed kernel width, the scheme performs online width adaptation based on the current coordination quality. Therefore, as the mismatch increases, the kernel function locally enhances its expressive power and naturally slows down its adjustment speed as the error decreases; the kernel center remains unchanged, thereby reducing the computational burden and simplifying the stability proof. Third, by introducing a small leakage term and forcing the parameters to be constrained within a certain range through projection or pruning operations, the weight learning law has anti-drift properties, preventing slow parameter drift under gusts or other disturbances that cannot be completely eliminated. In the implementation, each time step follows a clear local routine: assemble the network input from the local state, evaluate the Gaussian kernel of the current width, normalize the regressor, calculate the uncertainty estimate, update the width within a preset range, update the weights using leakage, and then project the weights back to the compact set; the total computational cost increases linearly with the number of kernels, so when the number of kernels is moderate, it can be executed on a single machine.

Table 1. Summary of the improved RBF design elements and implementation considerations

Design element	Why it is included	Main tuning knobs	Practical implementation note	Computation impact
Normalized basis regressor	Prevents regressor bursts during aggressive maneuvers; reduces	Normalization form, kernel count	Improves numerical stability in fixed-point	Small overhead
Online width adaptation	Improves approximation under time-varying uncertainties;	Width learning rate, lower width bounds	Keep centers fixed to simplify analysis; enforce width bounds by clipping	Linear in kernel count
Fixed kernel centers	Keeps learning stable and proof-friendly; reduces computation	Center placement strategy	Choose centers to cover expected operating region; grid or sampled trajectory points work well	No online cost beyond distance evaluation
Leakage in weight learning	Prevents slow weight drift under persistent disturbances	Leakage factor, weight learning rate	Too large leakage can reduce accuracy; too small may not suppress drift	Negligible overhead
Projection/clipping of weights	Guarantees bounded parameters for robustness and analysis	Weight bounds	Simple per-parameter clipping works in real-time; full projection improves rigor	Low to moderate
Local update routine	Makes the method reproducible and easy to implement	Sampling time, update ordering	Use the same error signal already computed for control; no extra communication needed	Overall linear in kernel count
Complexity profile	Ensures onboard feasibility	Kernel count, input dimension	Use a moderate kernel count; avoid high-dimensional inputs unless necessary	Roughly proportional to

3.3 Approximation Error Characterization and Discussion

With normalized basis functions and bounded widths, the regressor remains bounded over the operating domain [18]. Let Ωz denote the compact operating region of the UAV local state z_i. For the i-th UAV, the Gaussian basis function can be written as:

$$\phi_{ik}(z_i) = exp(\frac{\left\|z_i - c_{ik}\right\|^2}{-\sigma_{ik}^{\ 2}}) \tag{13}$$

Where c_{ik} is the center of the k-th basis function, $\sigma_{ik}^{\ 2}$ is the corresponding kernel width, and N denotes the number of RBF kernels. Since the kernel width is constrained within a preset bounded interval.

$$0 < \sigma_{min} \leq \sigma_{ik}(t) \leq \sigma_{max} \tag{14}$$

The basis function remains well-defined and avoids numerical singularity caused by excessively small widths or over-smoothing caused by excessively large widths. By using normalized basis functions and bounded widths, the regressor of the improved RBF neural network remains bounded within the operating domain, ensuring that the approximation error is characterized by a bounded residual term. This means that while the neural network cannot completely eliminate the uncertainties caused by a finite number of kernels, imperfect center positions, and external disturbances, the total approximation error can be constrained to an analyzable range. From a control perspective, the advantages of the proposed scheme are not only improved numerical approximation accuracy but

also that subsequent stability analysis is more manageable. First, normalization suppresses excessive increases in the basis function response during transient maneuvers, preventing the uncertainty compensation term from becoming excessively large and reducing the conservatism of the stability boundary. Without normalization, rapid changes in the UAV state could cause a rapid increase in the size of the regressor, expanding the upper limit of the approximation error and making the controller design more conservative. Second, width-constrained adaptation improves the transient matching ability of the model under various operating conditions. As the cooperative error increases, the kernel width can be adjusted online to improve local approximation ability. As errors decrease, tuning becomes smoother, helping to avoid unwanted oscillations in the basis functions. At the same time, fixing the kernel center reduces computational complexity and simplifies stability proofs. Thirdly, a leak term and projection mechanism are introduced into the weight update law to prevent gradual parameter drift under persistent disturbances, measurement noise, or residual approximation errors. This is particularly important for UAV formation control, as wind disturbances persist for long periods and cannot be completely canceled by the neural approximator. The proposed method ensures that both neural network parameters and approximation errors are constrained during the control process by restricting adaptive weights to a compact set. In the Lyapunov-based stability analysis, tuning errors and neural network weight estimation errors can be considered together, and it is shown that the derivative of the Lyapunov function is negative outside the bounded region. This indicates that the closed-loop system does not need to perfectly approximate all nonlinear uncertainties. Instead, it is sufficient to ensure that residual errors, parameter estimation errors, and disturbance-related terms are uniformly bounded. These characteristics are particularly important in formation stability analysis because transient adjustment errors can be amplified by network connectivity, and local errors in one UAV can affect neighboring UAVs through the communication topology. Therefore, by combining a normalized regressor, bounded width adaptation, leak learning, and projection constraints, the proposed improved RBF scheme provides a more robust uncertainty compensation mechanism. It improves transient approximation performance while maintaining the boundedness of the regressor, adaptive parameters, and residual approximation errors, and supports the derivation of a compact final stability boundary for UAV formation systems.

4 Design of a Stable Formation Control System

This section introduces a distributed formation controller that stabilizes a given formation by tracking the motion of the control module in Fig. 1. The design is based on a filtered formation error signal, allowing the closed-loop dynamics to be expressed in a form suitable for Lyapunov analysis. The improved RBF module introduced in Section 3 can compensate for unknown nonlinearities and model uncertainties in real time. Robust smoothing terms are introduced to reduce residual approximation errors and bounded disturbances. The overall concept adopts an explicit distributed design: each UAV only needs its own state and the states of its neighboring UAVs. This satisfies the practical requirements of multi-component system coupling.

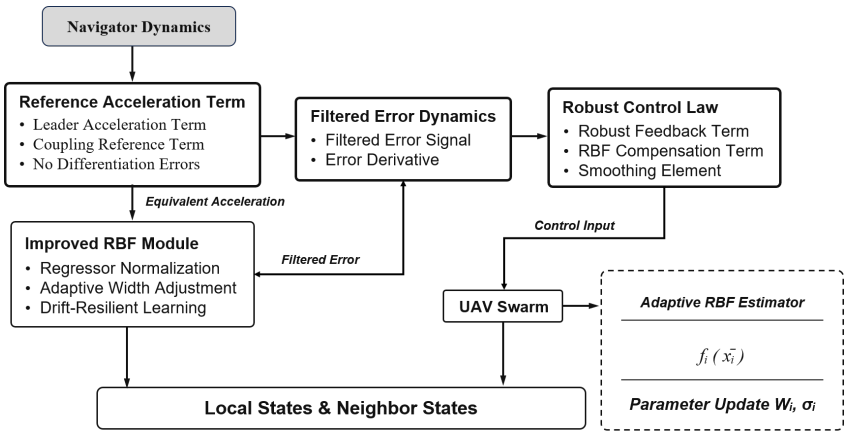

Fig. 1. Architecture of the distributed stable formation control system with improved RBF compensation

4.1 Preparation of Distributed Reference and Error Dynamics

To construct the controller, the objective function of the formation is first transformed into a local error system that can be computed by each UAV [19]. The local position error of the formation is determined by the relative positions of neighboring UAVs and the desired offset. Filtered variables are used to describe the position deviation and its rate of change. In practical applications, the filtered variables can be numerically calculated from the sampled signals or analytically derived from the error expression, taking velocity information into account. The filtered variables are the only feedback path to achieve stabilization. When this variable approaches zero, the local position error of the formation becomes a stable first-order system. This means that the position error converges to a near-zero point determined by the disturbance and approaches the residual. This is a common motivation for using filtered errors in adaptive and robust control systems, especially suitable for formation control, as it eliminates the need for efficient differentiation of the original position signal.

4.2 Control Structure and Basic Control Law

The proposed control input consists of four parts: a robust feedback element, an improved RBF compensation element, a robust smoothing element, and a feedforward control element caused by the motion of the lead UAV and the coupling of the formation [20]. The control law for UAV i is defined as follows.

$$u_i = B_i^{-1}(-K_i s_i - \hat{f}_i(x_i) - p_i sat(s_i / \delta_i) + a_{i,ref}) \tag{15}$$

Where u_i denotes the outer-loop control input of UAV i, and B_i denotes the known nonsingular input matrix in the UAV model. The vector s_i denotes the filtered formation error used for feedback stabilization. The matrix K_i denotes a positive definite feedback gain that shapes the convergence rate of the filtered error. The term $\hat{f}_i(x_i)$ denotes the online estimate of the unknown nonlinear term produced by the improved RBF approximator, where x_i is the local state used as the network input. The scalar p_i denotes the robust gain used to attenuate bounded disturbances and approximation residuals. The function sat denotes an element-wise saturation function, and sat denotes a small positive smoothing parameter. The vector $a_{i,ref}$ denotes an equivalent reference acceleration that collects known formation-coupling terms and leader-motion terms; it is constructed to avoid differentiating noisy signals and to keep the resulting error dynamics in a matched form. The smooth robust term is used instead of a discontinuous sign function to reduce chattering and actuator wear. A typical element-wise saturation function is defined as:

$$sat(y) = \begin{cases} y, \|y\| \le 1 \\ \dfrac{y}{\|y\|}, \|y\| > 1 \end{cases} \tag{16}$$

Where y denotes the input vector to the saturation nonlinearity. The saturation behaves linearly inside a boundary layer and smoothly transitions to a bounded direction-preserving output outside the boundary layer.

4.3 Construction of the Reference Acceleration Term

The reference acceleration term plays a crucial role in distinguishing between predictable movements and corrective movements generated by feedback control in formation flight. In formation flight, following aircraft must not only track the entire formation's flight path but also maintain a predetermined relative position to adjacent aircraft. Simultaneously, the navigator or lead aircraft may accelerate, decelerate, turn, or perform other maneuvers as required by their mission. If air traffic controllers do not explicitly consider these predictable movement elements, the feedback loop must simultaneously compensate for formation tracking errors and the navigator's normal maneuvering. In such situations, controllers may misinterpret the navigator's acceleration or predicted formation movements as external disturbances, resulting in excessive feedback gain, overly strong control inputs, and increased sensitivity to measurement noise, communication delays, and local estimation errors. Therefore, introducing a reference acceleration term allows controllers to distinguish between

spontaneous movements in the formation and movements that truly require correction. Within the framework of a navigator-follower formation, the reference acceleration term primarily contains two types of information. The first concerns the navigator's own movements. Since the navigator determines the overall movement tendency of the formation, the navigator's acceleration should be reflected in the predictable movement of the followers. When the navigator accelerates, decelerates, or changes direction, the followers should generate a corresponding acceleration response so that the entire formation moves in coordination, rather than simply treating and suppressing this movement as an error. In this sense, the navigator's acceleration provides a feedforward element to the followers, allowing them to predict the formation's movement tendency rather than relying entirely on delayed feedback correction. This is particularly important during sharp turns, velocity changes, and other transient maneuvers. The followers can react more smoothly, mitigating transient deformation of the formation. The second piece of information included in the reference acceleration term concerns the desired change in formation error. In formation control, the goal is not only to reduce instantaneous position deviations but also to control the dynamic process of convergence of relative position and velocity errors. Therefore, the reference acceleration term should be constructed to match the desired dynamic characteristics of the shape error. Ideally, in the absence of external disturbances, modeling errors, and communication failures, the coordination error filtered by this term should converge within the target region. This improves transient coordination, reduces formation distortion during maneuvering, and avoids excessive amplification of high-frequency noise. This is particularly important in real-world UAV systems because high feedback gains can make the controller overly sensitive to sensor noise, communication packet loss, and slight fluctuations in relative state measurements. Therefore, a properly designed reference acceleration term not only helps improve tracking accuracy, but also contributes to smoother control, more robustness, and greater actuator feasibility. From an implementation perspective, direct numerical differentiation of noisy position signals should be avoided when calculating the reference acceleration. Although shape errors are often determined using relative position, direct differentiation of position-based errors can introduce significant high-frequency noise. This problem is exacerbated in multi-agent systems, as relative information from neighboring aircraft may be subject to delays, quantization, intermittent updates, or temporary unavailability. Directly using such noisy differentiated signals in controllers can lead to control effects such as chatter and reduce the reliability of the swarm system. Therefore, it is more reliable to calculate error variations using available velocity information. Since the variation in relative position errors is primarily determined by relative velocity, using velocity signals provides a more stable and physically sound description of the error rate. If the navigator's acceleration cannot be measured directly, it should not be determined simply by differentiating the velocity signal, as this can also amplify measurement noise. Instead, smoothing differentiators, low-order observers, or filtered estimation methods can be used to obtain noise-insensitive estimates of the navigator acceleration. These methods offer a balanced ratio of performance to noise reduction and allow important maneuvering tendencies to be incorporated into the reference acceleration term without introducing excessive high-frequency components. This approach is particularly well-suited for practical UAV swarm systems where the accuracy and sampling rate of onboard sensors and communication modules are limited. Another important aspect is the decentralized computation of the reference acceleration term. This should be calculated using locally available information, such as the state of the following aircraft, relative information about the state of neighboring aircraft, and navigator-related information obtained through the communication topology. This avoids dependence on global swarm information and centralized computation, thereby increasing the scalability of the control strategy. Even with an increasing number of UAVs, each subsequent flight can calculate its own acceleration reference term based on local data, eliminating the need for a central controller to monitor and process the overall swarm state. This design is compatible with distributed formation control systems and is better suited for real-time implementation in large-scale UAV networks in Table 2.

Table 2. Functional role of the reference acceleration term in formation flight control

Aspect	Main content	Role in the control system
Control motivation	The reference acceleration term distinguishes predictable formation movements from corrective movements generated by feedback control.	Prevents the controller from treating navigator maneuvers as external disturbances.
Navigator motion information	The navigator may accelerate, decelerate, turn, or perform other mission-related maneuvers.	Provides a feedforward reference for followers so that the formation moves in a coordinated manner.

Aspect	Main content	Role in the control system
Formation error dynamics	The term reflects the desired change in formation error, including relative position and velocity error convergence.	Defines the nominal dynamic reference for the following aircraft.
Feedback loop reduction	Predictable navigator movements are considered in advance instead of being corrected only after tracking errors occur.	Reduces feedback burden, excessive gain, and overly strong control inputs.
Robustness improvement	High feedback gains may amplify sensor noise, communication delays, packet loss, and local estimation errors.	Improves smoothness, robustness, and actuator feasibility in practical UAV systems.
Acceleration estimation	Direct numerical differentiation of noisy position or velocity signals should be avoided.	Encourages the use of velocity information, smoothing differentiators, observers, or filtered estimation methods.
Decentralized implementation	Each follower calculates its reference acceleration using local states, neighbor states, and navigator-related information from the communication topology.	Avoids centralized computation and improves scalability for large-scale UAV networks.

4.4 Integration with the Improved RBF Module

The improved RBF module is added not as a general training component, but as an online compensator. Its output is estimates of the unknown dynamic parameters fed to the translational acceleration channel [21]. The controller can be thought of as having two layers: a distributed feedback layer to ensure convergence of the shaping and an adaptive compensation layer to reduce the uncertainty load on the feedback layer. Thanks to accurate RBF estimates, the feedback gain can be chosen more conservatively, the robustness term can be smaller, and the overall control input can be more uniform, while maintaining comparable or even higher shaping accuracy. A key design decision is the selection of network input signals. The guiding principle is to use a minimum number of signals capable of capturing the most significant uncertainties. For translational shaping control in the outer loop, local position and velocity are often sufficient, since many uncertainties and unaccounted effects manifest themselves as state-dependent acceleration errors. In more complex, uncertain environments, additional signals can be introduced to reflect the quality of the coordination. However, increasing the input data dimensionality typically requires a larger number of kernel functions to cover the operating range. This increases onboard computational costs and complicates the adaptation of learned dynamics. Therefore, low-dimensional input data is generally preferred unless performance constraints are significant. The advanced capabilities of the RBF module influence its interaction with the shaping controller in three ways. First, basis normalization prevents abrupt regressor changes during strong transients. This improves numerical behavior and prevents overfitting when the shaping temporarily deviates from the target conditions. Second, online width adjustment provides additional flexibility when the system enters new operating ranges or when uncertainty models change over time. This helps mitigate the mismatch problem often encountered with fixed-width kernel functions. Third, anti-drift learning prevents slow parameter divergence during long-term disturbances. This is especially important for long-duration shaping flights, where persistent disturbances are the rule rather than the exception. In practice, the RBF compensation output is computed at the same sampling rate as the controller. Parameter updates can use the same sampling rate or, if computing resources are limited, a slightly lower rate. A practical approach is to first calculate the compensation output based on the current parameters, then adjust the width within a specified range, and finally update the weights using a drift-prevention mechanism. This update sequence ensures that the compensation output remains stable and predictable at each time step. Importantly, the entire training process occurs exclusively within each drone and requires no additional communication beyond that necessary to generate shaping errors in Fig. 2.

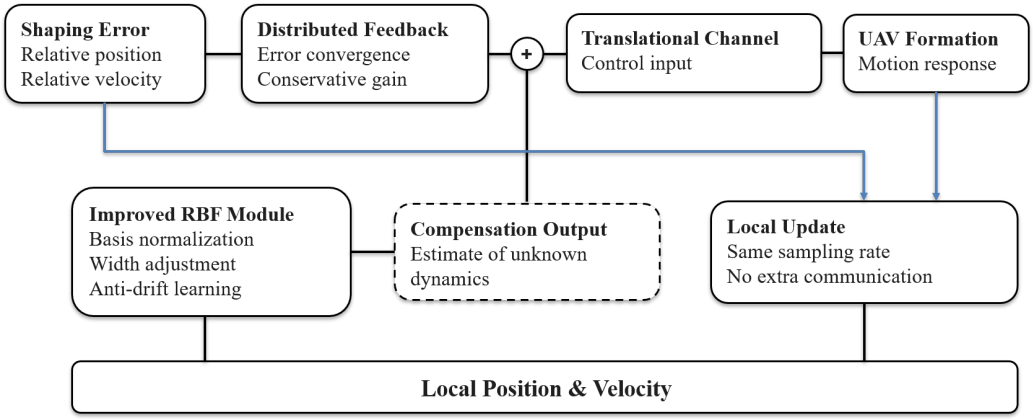

Fig. 2. Online RBF-Based adaptive compensation mechanism

5 Stability Analysis

A closed-loop stability analysis of the control system is performed by inferring the filtered error dynamics of each successive UAV within the proposed improved adaptive robust control law based on the radial basis function (RBF). In the closed-loop system, the filtered shaping error serves as the primary feedback variable, while the improved RBF neural network compensates for the unknown nonlinear dynamics, and a robust smoothing term suppresses residual approximation errors and limited external disturbances. By constructing a Lyapunov function that incorporates both the filtered error and the neural network weight estimation error, the proof demonstrates that the adaptive law can eliminate the primary parametrically dependent cross-term while adequately constraining the residual error, disturbances, and robust compensation terms. This leads to a dissipation inequality stating that the Lyapunov function decays outside a compact set of residuals. Thus, the filtered formation error, parameter estimation error and corresponding formation tracking errors are ultimately uniformly bounded, which proves that the proposed control scheme can ensure stable formation coordination of UAVs under the conditions of nonlinear uncertainties and external disturbances.

5.1 Closed-Loop Error Dynamics

Each UAV uses the filtered formation error as the primary feedback variable, and compensates for the unknown nonlinear terms in the translational motion state using an improved RBF estimate [22]. Substituting the control law and grouping terms, the filtered error dynamics of follower i can be written in standard matched uncertainty form:

$$\dot{s}_i = -K_i s_i + \tilde{W}_i^{\top} \bar{\Phi}_i(x_i) + \varepsilon_i(x_i) + d_i(t) - \rho_i sat(\frac{s_i}{\delta_i}) \tag{17}$$

Where s_i is the filtered formation error, and K_i is the stabilizing feedback gain matrix. The term $\bar{\Phi}_i(x_i)$ is the normalized RBF regressor evaluated at the local input x_i. The weight estimation error $\tilde{W}$ is defined as:

$$\tilde{W}_i = W_i - W_i^* \tag{18}$$

Where W_i is the online weight matrix and W_i^* is an ideal constant weight matrix associated with the normalized basis representation on the operating domain. The term $\varepsilon_i(x_i)$ captures the residual approximation error due to finite kernels and bounded width constraints, and $d_i(t)$ is the bounded external disturbance. The last term is a smooth robust action using a saturation nonlinearity; ρ_i is its gain and δ_i is the boundary-layer thickness parameter.

5.2 Lyapunov Function Candidate and Proof

A standard Lyapunov function that captures both tracking performance and parameter learning is chosen as:

$$V = \sum_{i=1}^{N} (\frac{1}{2} s_i^{\top} s_i + \frac{1}{2} tr(\tilde{W}_i^{\top} \Gamma_i^{-1} \tilde{W}_i)) \tag{19}$$

Proof Step 1: Differentiate the Lyapunov function.

$$\dot{V} = \sum_{i=1}^{N} (s_i^{\top} s_i + tr(\tilde{W}_i^{\top} \Gamma_i^{-1} \tilde{W}_i)) \tag{20}$$

Step 2: Use the adaptive law to cancel the cross term.

$$\dot{W}_i = -\Gamma_i \bar{\Phi}_i s_i^{\top} - \kappa_i W_i \tag{21}$$

Step 3: Bound the disturbance and residual terms.

$$\dot{W}_i = -\Gamma_i \bar{\Phi}_i s_i^{\top} - \kappa_i W_i \tag{22}$$

Step 4: Handle the smooth robust term.

$$-\rho_i s_i^{\top} sat(s_i / \delta_i) \le -\rho_i \|s_i\| + \rho_i c_i \delta_i \tag{23}$$

Step 5: Combine bounds and obtain a dissipation inequality.

$$\dot{V} \le -\alpha \sum_{i=1}^{N} \|s_i\|^2 + \beta \tag{24}$$

Step 6: Conclude UUB of the filtered error and formation error.

$$\sum_{i=1}^{N} \|si(t)\|^2 \le \alpha\beta \tag{25}$$

6 Simulation Studies

This section evaluates the proposed formation control strategy based on an improved RBF compensator under normal and stressed conditions. The simulations reproduce typical formation flight challenges, including parametric uncertainties, external wind disturbances, and a time-varying communication topology. The proposed method is compared with three baseline controllers to demonstrate that performance improvements are achieved through an optimized RBF design rather than overly aggressive feedback.

6.1 Simulation Setup and Test Scenarios

A UAV swarm is simulated using a translational motion model with unknown nonlinearities and bounded disturbances [23]. The formation target is defined by fixed target offsets, and the leader follows a smooth, time-varying trajectory. Each follower uses only information about its neighbors to calculate its local formation error and generate a control signal. Three scenarios are considered. Scenario S1 (Normal): The communication graph is stable and satisfies the leader-rooted tree condition. The leader follows a smooth reference trajectory, and

disturbances are negligible. This scenario tests baseline convergence and steady-state behavior. Scenario S2 (Parametric Uncertainty): The control system parameters in the follower dynamics are subject to disturbances. This scenario tests whether an improved RBF module can reduce the impact of the mismatch without high feedback gains. Scenario S3 (Disturbance+Topology Change): Wind gusts are introduced as temporally localized disturbances, and the communication topology changes at predetermined times. This scenario tests the resilience to persistent disturbances and network variability. To ensure fair comparison, the sampling time, simulation horizon and saturation limits remain the same for all controllers in all scenarios.

6.2 Results

This simulation study evaluates the performance of a proposed robust formation control strategy based on improved RBF compensation. Under nominal operating conditions, including parameter deviations and wind loads, the study is compared to representative baseline models to confirm that the performance improvement is due to the optimized RBF design rather than aggressive feedback adjustments. The experimental setup is first illustrated with a brief visualization of the directional linkage mode and the desired formation geometry. Links and links determine the information available to each UAV, as well as the relative target offset, which determines the formation shape in Fig. 3.

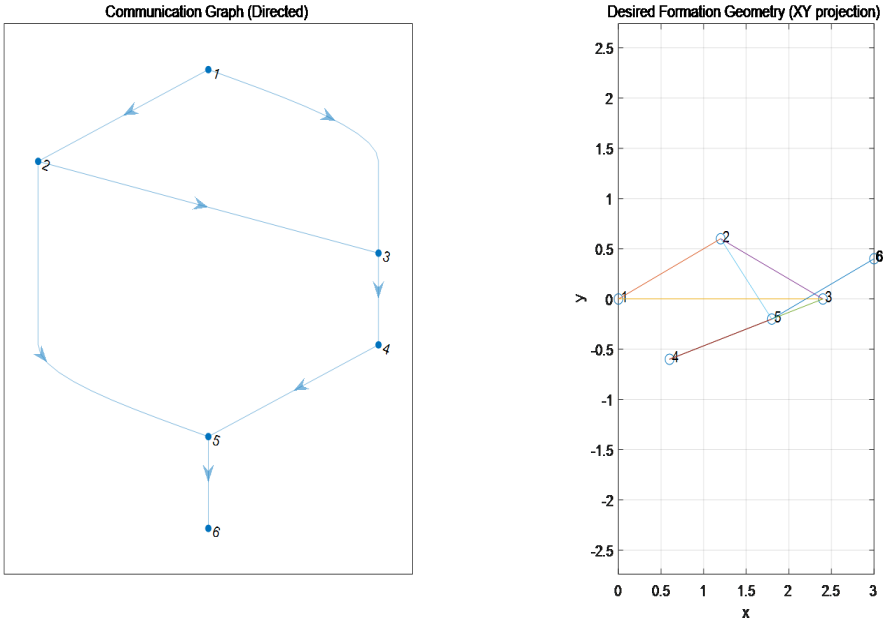

Fig. 3. Communication graph and desired formation geometry

In this setup, the navigator flies a single three-dimensional reference trajectory, while follower aircraft launch from dispersed launch sites. Using the proposed controller, the follower aircraft's trajectories converge to a consistent rigid body configuration that follows the navigator's motion without significant vibration propagation. The formation moves as a coordinated unit along the navigation trajectory, which can be directly observed from the package of navigation and follower trajectories in Fig. 4.

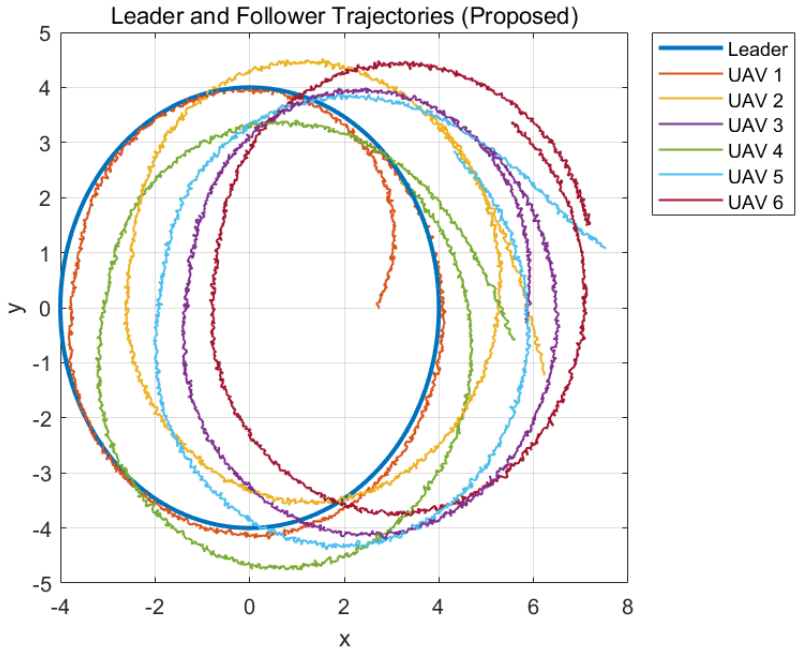

Fig. 4. 3D trajectories for the proposed method

To quantify the quality of coordination, this paper presents the aggregated norm of the formation error as a function of time for all methods. The results show that the proposed method provides faster error decay and a smaller steady-state region compared to the distributed matched baseline method, the traditional fixed-width RBF controller, and the robust SMC controller, especially during uncertain and perturbed phases in Fig. 5.

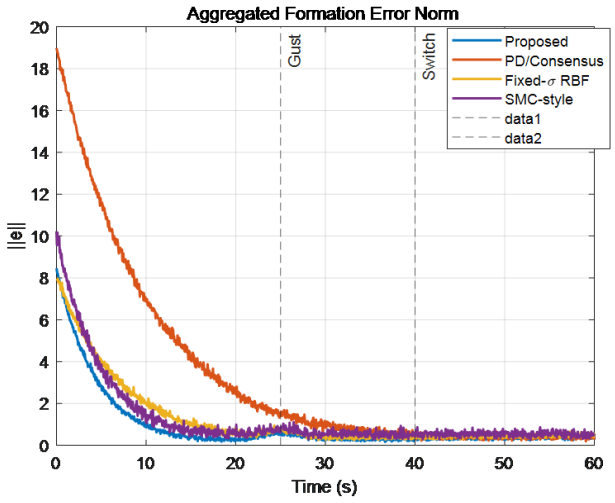

Fig. 5. Formation error norm comparison across methods

The control effect is investigated by plotting the aggregated norm of the controlled variable. The proposed method improves accuracy without increasing the input signal amplitude and reduces high-frequency activity compared to purely robust approaches. At the same time, compatibility with the actuator constraints is maintained, as shown by the saturation level in Fig. 6.

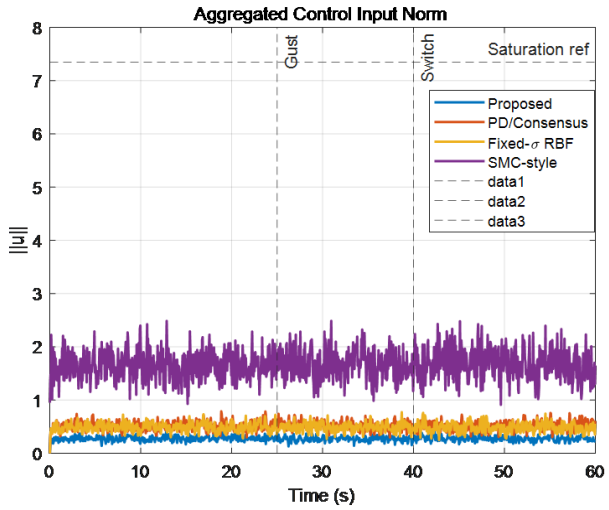

Fig. 6. Control input norm and saturation events

Since long-term shaping tasks are often affected by persistent winds, leading to adaptive parameter drift, the evolution of the neural network parameters was also monitored. Thanks to a drift-preventive learning mechanism, the weight norm remained bounded throughout the process; the width of the representative kernel adjusted primarily during short-term inconsistencies and then stabilized with improved coordination. This supports the hypothesis that width adjustment can improve expressiveness without compromising the stability of the learning process in Fig. 7.

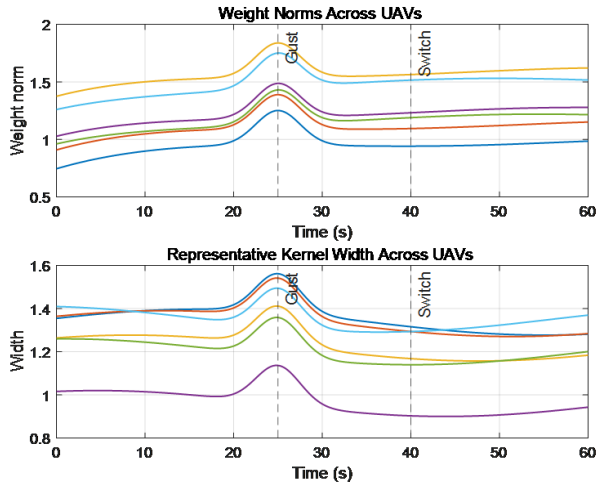

Fig. 7. Evolution of RBF weight norm and representative kernel width

Finally, robustness is emphasized by expanding the time window to account for the influence of wind gusts and changes in connection topology. During this period, the proposed method exhibits smaller error peaks and a higher recovery rate than the baseline method. This suggests that the combination of improved RBF compensation and smoothing robustness can effectively suppress rough residuals and external perturbations during network evolution in Fig. 8.

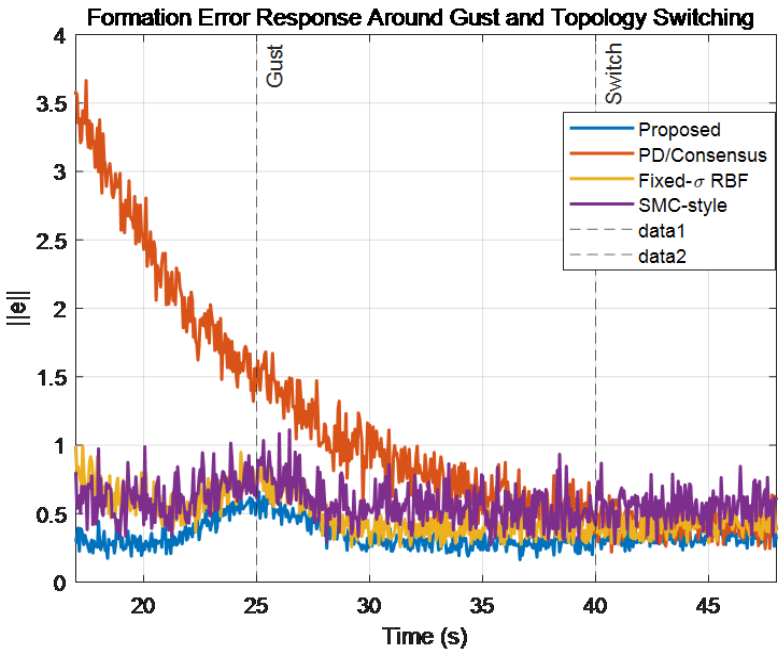

Fig. 8. Robustness test around gust injection and topology switching

7 Conclusions

This paper proposes a distributed robust shaping control strategy for multi-component UAV systems constrained by unknown nonlinear dynamics, finite external disturbances, and directional communication. Titled UAV Formation Stability Control Strategy Based on Improved Radial Basis Function, this strategy, based on locally computable shaping errors and filtered coordination variables, allows each follower to compute its control commands solely based on its own measurements and information received from its neighbors. Furthermore, the strategy allows for selective leader selection, ensuring the system's scalability and practical applicability. The main contribution lies in proposing an improved, radial basis function-based uncertainty compensator specifically designed for the shaping problem: regressor normalization suppresses transient spikes and improves numerical stability; finite online width adjustment enhances approximation capability under time-varying conditions; and an anti-drift learning mechanism ensures parameter constraints during long-term operation under continuous disturbances. By combining this training module with a stable backbone network and robust smoothing elements, the controller reduces the uncertainty load on the feedback loop, suppresses residual approximation errors and wind disturbances, prevents fluctuations, and ensures high control accuracy. Using Lyapunov analysis, we prove the constraints on all signals in the closed-loop control system, as well as the uniform finite constraint on the generated error. This reveals the dependence of steady-state control accuracy on disturbance level, residual approximation error, and boundary layer smoothing, thus providing a theoretical basis for practical applications. Comprehensive simulation results, including visualization of link topology and formation geometry, 3D master-slave trajectory tracking, comparison of fault curves and control curves, adaptive parameter evolution monitoring, and robust gain testing under gusts and topology changes, consistently demonstrate that compared to typical basic controllers, this method exhibits faster convergence, a smaller steady-state fault environment, and better stress handling capabilities. This highlights the effectiveness and robustness of the proposed method in achieving stable UAV swarm formations under uncertain conditions.

8 Acknowledgement

S&T Program of Xingtai: Research and Application of Stability Control in UAV Formation Flight (2026ZC029).

References

[1] S.-N. Alkhamees, S.-A. Alsaif, Y.-B. Salamah, Recent advances and a hybrid framework for cooperative UAV formation control, Applied Sciences 15(17)(2025) 9761.1-9761.18.
https://doi.org/10.3390/app15179761

[2] D. Debnath, F. Vanegas, J. Sandino, A.-F. Hawary, F. Gonzalez, A review of UAV path-planning algorithms and obstacle avoidance methods for remote sensing applications, Remote Sensing 16(21)(2024) 4019.1-4019.35.
https://doi.org/10.3390/rs16214019

[3] A. Farooq, Z.-G. Xiang, W.-J. Chang, M.-S. Aslam, Recent advancement in formation control of multi-agent systems: A review, Computers, Materials & Continua 83(3)(2025) 3623-3674.
https://doi.org/10.32604/cmc.2025.063665

[4] M. Chang, J.-S. Zhou, D.-X. Tian, X.-T. Duan, K.-G. Qu, D.-P. Cao, Uncertainty-aware robust UAV trajectory planning with dynamic collision avoidance, IEEE Internet of Things Journal 12(17)(2025) 36502-36516.
https://doi.org/10.1109/JIOT.2025.3582721

[5] L. Zhao, L.-W. Dai, Y.-Q. Xia, P. Li, Attitude control for quadrotors subjected to wind disturbances via active disturbance rejection control and integral sliding mode control, Mechanical Systems and Signal Processing 129(2019) 531-545.
https://doi.org/10.1016/j.ymssp.2019.04.040

[6] G. Wang, Z.-Y. Zuo, Consensus control of multi-agent systems with different state constraints and event-triggered communication, IEEE Transactions on Circuits and Systems II: Express Briefs 71(2)(2024) 817-821.
https://doi.org/10.1109/TCSII.2023.3314647

[7] C. Peng, Y. Bai, X. Gong, Q.-J. Gao, C.-J. Zhao, Y.-T. Tian, Modeling and robust backstepping sliding mode control with adaptive RBFNN for a novel coaxial eight-rotor UAV, IEEE/CAA Journal of Automatica Sinica 2(1)(2015) 56-64.
https://doi.org/10.1109/JAS.2015.7032906

[8] J. He, B.-W. Ren, Y.-S. Xu, Q.-J. Zhao, S.-L. Du, B. Wang, Neural network adaptive attitude control of full-states quad tiltrotor UAV, Aerospace 12(8)(2025) 684.1-684.27.
https://doi.org/10.3390/aerospace12080684

[9] Y. Wang, Z.-B. Du, Data-driven fault-tolerant bipartite consensus for multiagent systems with directed topology, IEEE Systems Journal 19(2)(2025) 425-434.
https://doi.org/10.1109/JSYST.2025.3540722

[10] P. Pal, R.-K. Behera, R. Sharma, Fast integral terminal sliding mode control based current sensorless scheme of DAB converter, IEEE Transactions on Industry Applications 61(4)(2025) 6593-6604.
https://doi.org/10.1109/TIA.2025.3550105

[11] D.-D. Wang, Q. Zong, B.-L. Tian, F. Wang, L.-Q. Dou, Finite-time fully distributed formation reconfiguration control for UAV helicopters, International Journal of Robust and Nonlinear Control 28(18)(2018) 5943-5961.
https://doi.org/10.1002/rnc.4361

[12] G.-Q. Zhang, J. Han, J.-Q. Li, X.-K. Zhang, Distributed robust fast finite-time formation control of underactuated ASVs in presence of information interruption, Journal of Marine Science and Engineering 10(11)(2022) 1775.1-1775.18.
https://doi.org/10.3390/jmse10111775

[13] D.-H. Yan, W.-G. Zhang, H. Chen, J.-P. Shi, Robust control strategy for multi-UAVs system using MPC combined with Kalman-consensus filter and disturbance observer, ISA Transactions 135(2023) 35-51.
https://doi.org/10.1016/j.isatra.2022.09.021

[14] B.-W. Fei, W.-D. Bao, X.-M. Zhu, D.-Q. Liu, T. Men, Z.-L. Xiao, Autonomous cooperative search model for multi-UAV with limited communication network, IEEE Internet of Things Journal 9(19)(2022) 19346-19361.
https://doi.org/10.1109/JIOT.2022.3165278

[15] Z.-W. Bai, G.-Y. Wu, M.-J. Barth, Y.-K. Liu, E.-A. Sisbot, K. Oguchi, Z.-T. Huang, A survey and framework of cooperative perception: From heterogeneous singleton to hierarchical cooperation, IEEE Transactions on Intelligent Transportation Systems 25(11)(2024) 15191-15209.
https://doi.org/10.1109/TITS.2024.3436012

[16] M.-L. Trinh, D.-T. Nguyen, L.-Q. Dinh, M.-D. Nguyen, D.-R.-I.-M. Setiadi, M.-T. Nguyen, Unmanned aerial vehicles (UAV) networking algorithms: Communication, control, and AI-based approaches, Algorithms 18(5)(2025) 244.1-244.62.
https://doi.org/10.3390/a18050244

[17] Y.-J. Lin, Z.-Y. Lin, Z.-Y. Sun, B.-D.-O. Anderson, A unified approach for finite-time global stabilization of affine, rigid and translational formation, IEEE Transactions on Automatic Control 67(4)(2022) 1869-1881.

https://doi.org/10.1109/TAC.2021.3084247
[18] S.-J. Fu, Y.-J. Tian, L. Tang, Robust regression under the general framework of bounded loss functions, European Journal of Operational Research 310(3)(2023) 1325-1339.
https://doi.org/10.1016/j.ejor.2023.04.025
[19] J.-Y. Tian, R.-X. Wei, L.-T. Jiang, Formation construction and reconfiguration control of UAV swarms: A perspective from distributed assignment and optimization, Nonlinear Dynamics 112(2024) 21171-21191.
https://doi.org/10.1007/s11071-024-10024-z
[20] S.-J. Kim, J.-H. Suh, Model-free RBF neural network intelligent-PID control applying adaptive robust term for quadrotor system, Drones 8(5)(2024) 179.1-179.17.
https://doi.org/10.3390/drones8050179
[21] M.-A.-D. Alves, J.-O.-P. Pinto, L. Galotto, M.-L.-M. Kimpara, R.-C. Garcia, R.-B. Godoy, A modified algorithm for training and optimize RBF neural networks applied to sensor measurements validation, IEEE Sensors Journal 21(17) (2021) 18990-18999.
https://doi.org/10.1109/JSEN.2021.3087107
[22] P.-F. Yu, Q. Li, Fully distributed low-complexity UAV formation control with fixed-time full-state error performance, IEEE Access 13(2025) 68224-68231.
https://doi.org/10.1109/ACCESS.2025.3557921
[23] A. Phadke, F.-A. Medrano, C.-N. Sekharan, T. Chu, Designing UAV swarm experiments: A simulator selection and experiment design process, Sensors 23(17)(2023) 7359.1-7359.26.
https://doi.org/10.3390/s23177359